Materials Advances

ROYAL SOCIETY OF CHEMISTRY

REVIEW

View Article Online
View Journal | View Issue

Cite this: *Mater. Adv.*, 2022, 3, 6742

LAPONITE® nanodisk-based platforms for cancer diagnosis and therapy

Gaoming Li,[a] Yunqi Guo,[a] Rui Guo,[a] Xiangyang Shi *[ab] and Mingwu Shen *[a]

Received 4th June 2022,
Accepted 16th July 2022

DOI: 10.1039/d2ma00637e

rsc.li/materials-advances

Recent advances in nanomedicine are rapidly extending the boundaries of biomedical technologies, particularly in tumor diagnosis and therapy. As a typical two-dimensional nanomaterial, LAPONITE® (LAP) has attracted much attention due to its good biocompatibility, colloidal stability, high specific surface area, and easiness of surface functionalization. Considerable progress has been made in the development of various LAP-based nanoplatforms for tumor diagnosis, treatment, and theranostics. In this review, we survey the recent advances in the development of various LAP-based drug delivery systems that have been used for tumor chemotherapy and phototherapy, tumor imaging, and tumor theranostics. The challenges and future development strategies for LAP-based nanomedicines toward practical biomedical applications are also discussed.

1. Introduction

Cancer is a major public health problem worldwide with a high mortality rate. Traditional cancer treatment methods including chemotherapy, radiotherapy and surgery have serious side effects or cannot completely eliminate tumors.[1–3] As a modern technology combining the characteristics of nanomaterials and the therapeutic effects of payload, nanotechnology has been extensively investigated and has been considered to revolutionize the traditional treatment of cancer.[4–6] To date, a few nanoagents have been approved by the Food and Drug Administration (FDA) for the clinical treatment of cancer or are in different stages of clinical studies, such as Doxil®, Abraxane®, NanoTherm®, and Atu027.[7,8] In preclinical studies, combined with the physiological characteristics of tumor cells and tumor microenvironments (TME), such as overproduction of hydrogen peroxide (H_2O_2) and glutathione (GSH), hypoxia, weak acidity, overexpression of enzymes, *etc.*,[9] nanomedicines play an increasingly important role in some of the latest cancer treatment methods developed in recent decades, such as sonodynamic therapy (SDT), phototherapy, chemodynamic therapy (CDT), immunotherapy and so on.[10–16]

For nanomedicine development, it is inevitable to choose a suitable nanomaterial as a platform. Various nanomaterials including organic nanomaterials such as liposomes, micelles, dendrimers, polymers, *etc.*[17–22] and inorganic nanomaterials such as ultrasmall iron oxide (Fe_3O_4), gold, silica (SiO_2), layered double hydroxide (LDH), LAPONITE® (LAP) nanoparticles (NPs), *etc.*[5,23–25] have been extensively explored. These reported organic and inorganic nanomaterials have different structural compositions and properties, and their applications in tumor diagnosis and treatment have been widely studied. For example, organic nanomaterials such as liposomes have high efficiency in gene delivery, iron oxide NPs have excellent magnetic resonance imaging capabilities, and gold NPs can be used for photothermal therapy and computed tomography (CT) imaging of tumors. In addition to their respective advantages, some of the nanomaterials also have some disadvantages, such as complex synthesis steps, high cost, difficulty to control their morphology and long-term toxicity *in vivo*. Among various nanomaterials, LAP is a synthetic smectite clay with structure and composition closely resembling the natural clay mineral hectorite. It is a layered hydrous magnesium silicate belonging to the family of (2 : 1) phyllosilicates built up of sheets of octahedrally coordinated magnesium oxide sandwiched between two parallel sheets of tetrahedrally coordinated silica.[26] The empirical formula of LAP is $Na^+_{0.7}[(Si_8Mg_{5.5}Li_{0.3})O_{20}(OH)_4]^{-0.7}$ showing the presence of oxygen atoms and OH groups, and some magnesium atoms are substituted by lithium forming a net negative charge that is balanced by interlayer sodium ions. LAP can be dispersed in water as nanodisks (NDs) with a diameter of 25 nm and a thickness of 0.92 nm to form a colloidal dispersion. The release of Na^+ ions results in a negative surface charge, while the protonation of the OH groups located at the edge of the disk results in a positive charge.[24,27,28] LAP has attracted extensive research interest in cosmetics and biomedicine due to its easy mass production, low cost, desired purity, and controlled

[a] *State Key Laboratory for Modification of Chemical Fibers and Polymer Materials, Shanghai Engineering Research Center of Nano-biomaterials and Regenerative Medicine, College of Biological Science and Medical, Engineering, Donghua University, Shanghai 201620, P. R. China. E-mail: mwshen@dhu.edu.cn, xshi@dhu.edu.cn*

[b] *CQM – Centro de Química da Madeira, Universidade da Madeira, Campus da Penteada, 9020-105 Funchal, Portugal*

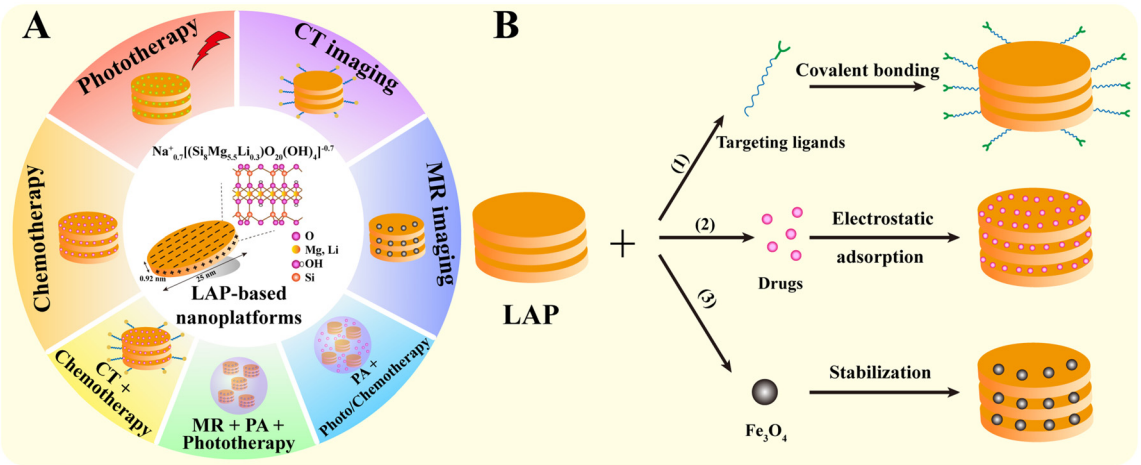

Fig. 1 (A) Schematic illustration of LAP-based nanoplatforms in cancer nanomedicine applications. (B) Preparation of LAP-based nanoplatforms by (1) covalent surface modification, (2) physical encapsulation or interaction, and (3) stabilization with biological substances or NPs.

composition.[29–31] Furthermore, LAP has been shown to be degradable, especially under acidic conditions, releasing degraded products such as aqueous silica ($Si(OH)_4$), sodium, magnesium and lithium ions into the solution, and has good biocompatibility.[24]

As a typical two-dimensional nanomaterial with large specific surface area, good biocompatibility, biodegradability, colloidal stability and easiness of chemical modification, LAP has been well explored in the biomedical field, especially in the diagnosis and treatment of tumors.[32–34] Recent efforts have been largely devoted to the development of a range of new LAP-based nanoplatforms for tumor diagnosis, treatment and theranostics. Therefore, in this review, we attempt to summarize the progress of the LAP-based nanoplatforms for cancer nanomedicine applications and discuss the opportunities and challenges to further advance the use of LAP nanoplatforms for clinical translation (Fig. 1A). It should be noted that this is not an extensive overview of all aspects associated with LAP-based cancer nanomedicines, but rather a discussion on the recent developments of the key advances in the associated research progresses in the past 5 years.

2. Preparation of LAP-based nanoplatforms

The structural characteristics and chemical modifiability of LAP are the prerequisites for the preparation of LAP-based nanoplatforms. Functional LAP-based nanoplatforms can be prepared by (1) covalent surface modification, (2) physical encapsulation or interaction, and (3) stabilization with biological substances or NPs.

2.1. Covalent surface modification

LAP NDs can be covalently functionalized through their surface silanol groups with monofunctional and trifunctional alkoxysilanes. Most of the work has been focused on the surface amination of LAP NDs to render them with a wide range of derivatization opportunities. For instance, LAP NDs can be surface silanized with 3-aminopropyltrimethoxysilane (APMES) to yield 4–14% organic coating. With APMES amines on the surface of LAP NDs, the NDs can be further attached to methacrylate, benzophenone, and tertiary bromine groups capable of polymerization, photoinitiation, and atom transfer radical polymerization initiation, respectively.[35] Tumor-targeting molecules and contrast agents can also be modified on the surface of LAP NDs by covalent bonding to endow them with targeting specificity and contrast enhancement, respectively (Fig. 1B(1)). For example, Wu *et al.* reported an LAP-based nanoplatform covalently modified with folic acid (FA) for tumor-targeted delivery. Aminated LAP NDs were first prepared by silanization, and then functionalized with polyethylene glycol-linked FA (PEG-FA) *via* 1-ethyl-3-(3-dimethylaminopropyl) carbodiimide hydrochloride (EDC) chemistry.[36]

2.2. Physical encapsulation or interaction

Non-covalent functionalization of LAP is mainly based on electrostatic interactions. Here, the interaction between polar molecules or molecular ions existing in the environment and the negative charge on the surface of clay or the positive charge on the edge of clay takes place.[24] For example, our group reported that DOX can be intercalated into the interlayer space of LAP NDs by an ionic exchange process (Fig. 1B(2)).[27]

2.3. Stabilization

Some contrast agents, such as Fe_3O_4 NPs, are prone to aggregation due to their large surface area and strong magnetic properties. Various stabilizers, such as chitosan, polyethylenimine (PEI), dendrimers, and peptides, provide the desired colloidal stability of Fe_3O_4 NPs. Unfortunately, the use of these stabilizers typically results in a significant reduction in the T_2 relaxation rate and reduced contrast enhancement in magnetic resonance (MR) imaging compared to the naked Fe_3O_4 NPs. In our earlier work, we reported the use of LAP as a stabilizer of Fe_3O_4 NPs for MR imaging of tumors by a facile controlled coprecipitation route in the presence of LAP. The formed LAP–Fe_3O_4 NPs have great

colloidal stability and about 2-fold increase of r_2 relaxivity than naked Fe_3O_4 NPs (Fig. 1B(3)).[37]

3. LAP nanoplatforms for cancer therapy

Chemotherapy is still a common method for cancer therapy, but the commonly employed anticancer drugs suffer problems of poor water solubility, low selectivity and undesirable side effects.[38,39] LAP NDs can be used as nanocarriers for the delivery of a wide range of therapeutic drugs due to the fact that they can be tailored to have different surface modifications and have different ways to encapsulate drugs, providing many promising opportunities for enhanced anticancer drug delivery applications. In addition, phototherapy has also been developed with high efficiency, low invasiveness, and few side effects.[40–42] Besides the use of LAP nanoplatforms for cancer chemotherapy, small molecular photosensitizers can also be efficiently loaded for phototherapy and combination therapy of cancer.

3.1. Cancer chemotherapy

Small molecular chemotherapeutic drugs have drawbacks in the clinical treatment of tumors, and the long-term use of high-dose chemotherapeutic drugs is likely to cause drug resistance in tumor tissues.[39] The side effects and the multidrug resistance (MDR) of the tumors seriously compromise the bioavailability of the drugs, thus affecting their therapeutic efficacy.[43] LAP NDs have several advantages, including the ability to transport drugs with high payloads, extended drug half-life, reduced drug toxicity, and improved targeting efficiency. Therefore, the LAP nanoplatforms, as carriers for delivering chemotherapeutic agents, have been designed to overcome side effects and MDR by improving drug water-solubility, colloidal stability, controlled drug release properties, tumor-targeting specificity, and multidrug combinations.[44,45]

In an early attempt, we first employed LAP NDs as a platform to effectively deliver anticancer drug doxorubicin (DOX) to cancer cells (Fig. 2A).[27] We showed that DOX was intercalated into the interlayer space of LAP NDs by an ionic exchange process and the DOX loading efficiency was up to 98.3%. The formed LAP/DOX nanocomplexes released DOX in a pH-dependent manner, and the release rate was faster under slightly acidic conditions (pH 5.4) than under physiological conditions (pH 7.4) (Fig. 2B). Importantly, the cell viability assay results revealed that, under the same concentration of DOX, the LAP/DOX nanocomplexes had a much stronger inhibitory effect on the growth of KB cells (a human epithelial carcinoma cell line) than free DOX due to the much more cellular uptake of the LAP/DOX nanocomplexes than free DOX (Fig. 2C). Similarly, Goncalves *et al.* employed alginate (AG), a biocompatible and degradable natural polymer, to coat LAP NDs for DOX loading.[46] The formed LAP/DOX/AG nanohybrids with a high DOX encapsulation efficiency of 80.8% could release DOX in a pH-sensitive manner and displayed a sustained drug release behavior. The cell experiment

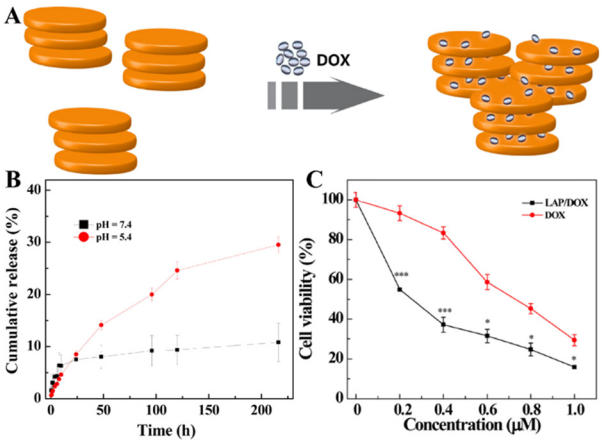

Fig. 2 (A) Schematic illustration of the intercalation of DOX into LAP. (B) *In vitro* release of DOX from LAP/DOX NDs at 37 °C under different pH conditions (pH = 5.4 and 7.4). (C) *In vitro* MTT viability assay of KB cells treated with LAP/DOX NDs and free DOX at different DOX concentrations for 24 h. Reproduced with permission.[27] Copyright 2013, American Chemical Society.

results indicated that the LAP/DOX/AG nanohybrids were an excellent nanoplatform for enhanced anticancer drug delivery applications.

The colloidal stability of nanomaterials is critical for their improved biomedical applications. In order to improve the colloidal stability of LAP NDs, Wang *et al.* developed stable LAP-based nanohybrids through the functionalization of the LAP surface with an amphiphilic poly(ethylene glycol)–poly(lactic acid) (PEG–PLA) di-block copolymer by a self-assembly process (Fig. 3A).[47] The resulting nanocarriers could be effectively loaded with the DOX drug to have a loading efficiency of 85.0% and displayed a pH-sensitive drug release behavior in a sustained way. The use of the PEG–PLA copolymer to assemble onto the surface of LAP NDs could improve their stability under physiological conditions (Fig. 3B and C). However, the inert structure of PEG–PLA also caused a decrease in both the drug loading capacity and pH sensitivity for drug release. Precise control of the drug release from nanocarriers could be beneficial for tumor treatment. To achieve this goal, the preformed DOX/LAP nanohybrids coated with cationic poly(allylamine) hydrochloride and anionic poly(sodium styrene sulfonate) multilayers through the electrostatic layer-by-layer self-assembly approach were developed by Xiao and coworkers.[48] The results showed that the presence of the polyelectrolyte multilayers improved the sustained release properties of LAP nanocarriers and allowed a fine tuning of the extension of drug release under neutral and acidic pH conditions. In addition, poly(N-vinylpyrrolidone) (PVP) was used to stabilize DOX-loaded LAP NDs by the interaction of the hydrophobic component (alkane polymeric chain) of PVP with the hydrophilic components (ketone and tertiary amine residues) of the LAP surface. *In vitro* drug release experiments showed that DOX could be released from the LAP/DOX/PVP nanohybrids with dual pH and thermal sensitivity.[49] To overcome the MDR of tumors, it is very important to develop a drug delivery system that can effectively

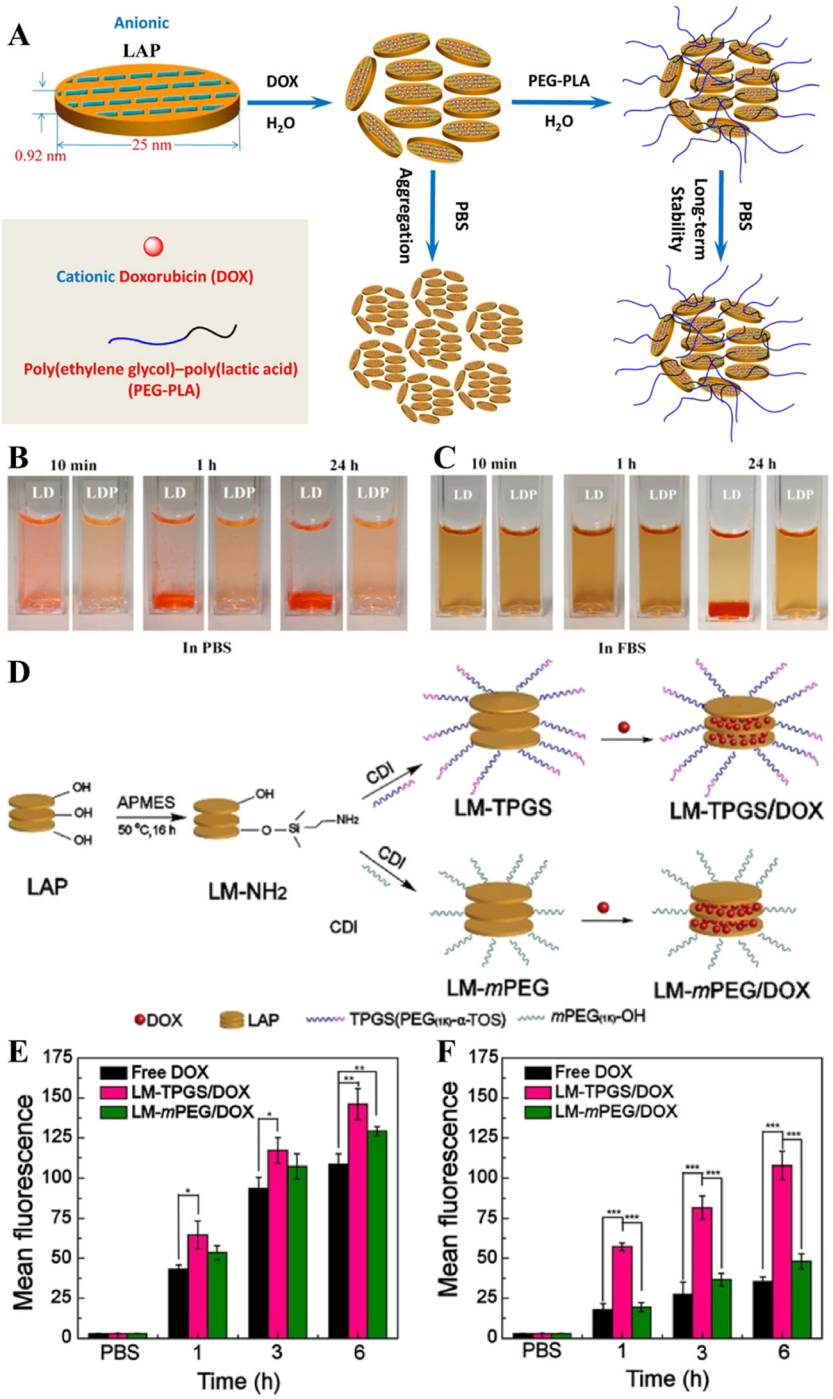

Fig. 3 (A) Schematic representation of the fabrication of LP/DOX (LD nanocomplexes) and LP/DOX/PEG–PLA (LDP nanohybrids) nanocarriers. The dispersed state of LD or LDP in (B) phosphate buffered saline (PBS) and (C) fetal bovine serum. Reproduced with permission.[47] Copyright 2014, American Chemical Society. (D) Schematic illustration of the synthesis of LM–TPGS/DOX. Flow cytometry measurements of the intracellular uptake of MCF-7 cells (E) and MCF-7/ADR cells (F) incubated with DOX-loaded NDs using the same dose (C_{DOX} = 7.5 μg mL^{-1}) for 1 h, 3 h, and 6 h, respectively. Reproduced with permission.[50] Copyright 2020, Wiley-VCH.

load two or more chemotherapeutic drugs. Zhou *et al.* developed a nanoplatform with first DOX loading onto the surface of LAP NDs, then with PVP polymer coating, and finally with the loading of mitoxantrone, another chemotherapy drug by self-assembly.[44] The formed dual-drug delivery system had good colloidal stability with a high drug encapsulation efficiency, and presented a sequential release profile of the two drugs with the drug release rate accelerated under an acidic TME. In addition, P-glycoprotein (P-gp)-mediated drug efflux has been considered to be an important mechanism for MDR. To overcome the MDR of tumors, Jiang *et al.* first modified APMES on the surface of LAP NDs to introduce amines, then

conjugated d-α-tocopheryl polyethylene glycol (PEG) 1000 succinate (TPGS), a kind of P-gp inhibitor onto the LAP surface, and finally loaded DOX within the nanohybrids by physical adsorption (Fig. 3D).[50] *In vitro* and *in vivo* experiments showed that the formed LM/TPGS/DOX nanohybrids could be taken up by DOX-resistant breast cancer cells (MCF-7/ADR) and exhibit the enhanced antitumor efficacy by inhibiting the activity of P-gp-mediated drug efflux (Fig. 3E and F).

Although nanomaterials can passively target tumor tissues through the known enhanced permeability and retention (EPR) effect, the efficiency of passive tumor targeting is very limited. Therefore, it is vital to develop nanocarrier systems with the active targeting specificity to further improve the antitumor effect of nanomedicines. In order to realize the active tumor targeting effect of the nanoplatform, targeting ligands are generally modified onto the surface of the nanoplatforms. In terms of LAP NDs, galactose-bearing lactobionic acid (LA) has been exploited as a targeting agent to realize targeted anticancer drug delivery to cancer cell overexpressing asialoglycoprotein receptors (ASGPRs). In a work by Chen *et al.*, LAP NDs were covalently modified with PEG-linked lactobionic acid (PEG-LA) and then were efficiently loaded with DOX.[52] *In vitro* flow cytometry and confocal laser scanning microscopic observation showed that the developed LM–PEG–LA/DOX nanohybrids could be employed for targeted DOX delivery to HepG2 cells with the targeting specificity much higher than the control LA-free LM-*m*PEG/DOX nanohybrids. Similarly, the LAP surface can also be covalently modified with hyaluronic acid (HA) and loaded with DOX (Fig. 4A) for targeted drug delivery to cancer cell overexpressing CD44 receptors.[51] For better cancer cell targeting, Yang *et al.* developed a DOX/LAP/HA-PBA nanoplatform that can effectively target MCF cells for DOX delivery using

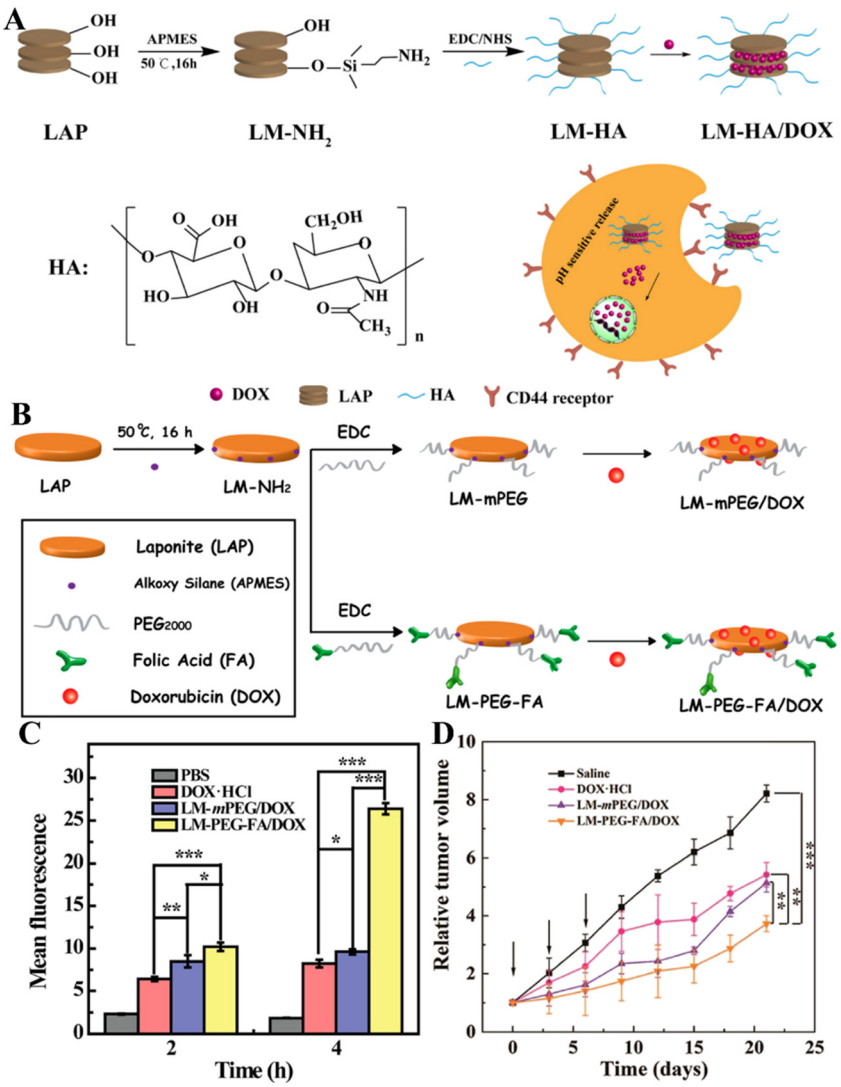

Fig. 4 (A) Schematic illustration of the preparation of LM–HA/DOX. Reproduced with permission.[51] Copyright 2019, MDPI. (B) Illustration of the synthesis of LM-*m*PEG and LM–PEG–FA for DOX encapsulation. (C) The mean fluorescence intensity of SK-OV-3 cells after treatment with different materials for 2 and 4 h, respectively. (D) Relative tumor volume change of tumor-bearing mice after different treatments. Reproduced with permission.[36] Copyright 2020, American Chemical Society.

LAP NDs coated with synthetic HA-phenylboric acid (PBA), where both HA and PBA can act as targeting ligands to specifically target the CD44 receptor and sialic acid, respectively, that are overexpressed by cancer cells.[53] In a very recent work, Wu *et al.* reported an LAP-based nanoplatform modified with PEG–FA and loaded with DOX (Fig. 4B) for targeted drug delivery to cancer cells (SK-OV-3 cells, a human ovarian cancer cell line) *in vitro* (Fig. 4C) and a subcutaneous tumor model *in vivo*.[36] The *in vivo* results showed that the LM–PEG–FA/DOX nanocomplexes had a much stronger inhibitory effect on the SK-OV-3 xenograft model than the control FA-free LM-*m*PEG/DOX nanocomplexes (Fig. 4D). In addition, the results of H&E staining of major organs (heart, liver, spleen, lung, and kidney) showed that the major organs of tumor-bearing mice treated with LM–PEG–FA/DOX had no obvious damage, indicating that the formed LM–PEG–FA/DOX has good biocompatibility.

3.2. Cancer photothermal and photodynamic therapies

With the development of cancer nanomedicine, some new treatment methods have attracted more and more attention, such as photothermal therapy (PTT), photodynamic therapy (PDT), CDT, SDT, and gas therapy.[12,54,55] LAP NDs have been developed to create different nanoplatforms to exert PTT and PDT of tumors.

PTT and PDT are emerging physical tumor treatment modes utilizing near infrared (NIR) light-absorbing agents for the thermal ablation of cancer cells or for the generation of highly toxic reactive oxygen species (ROS) *via* photosensitizers to kill cancer cells.[56] PTT and PDT possess several advantages, such as minimal invasion, high therapeutic efficacy, limited side-effects, and selective localized treatment.[57] Indocyanine green (ICG) is an excellent agent for both PTT and PDT of cancer cells since it can effectively convert the absorbed NIR laser light into heat for PTT and produce ROS for PDT under NIR laser irradiation. In a recent work, Xu *et al.* developed a novel nanoplatform (denoted as ICG/LAP–PDA–PEG–RGD) through the coating of polydopamine (PDA) onto the ICG-loaded LAP NDs and then further conjugating the PEGylated arginine–glycine–aspartic acid sequence (PEG-RGD) as a targeting agent onto the particle surface (Fig. 5A).[57] The ICG/LAP–PDA–PEG–RGD platform enabled combined specific PTT and PDT treatments of cancer cell overexpressing integrin $\alpha_v\beta_3$.

In general, a single PTT treatment usually requires a higher laser power density, and a single PDT treatment usually requires a higher photosensitizer dose. In order to reduce the laser power density and limit the dose of photosensitizers, Wu *et al.* synthesized an LAP-based nanoplatform by *in situ* polymerization of pyrrole to form polypyrrole-loaded LAP NDs (for short, LP), and then coating of the LP with PVP to create

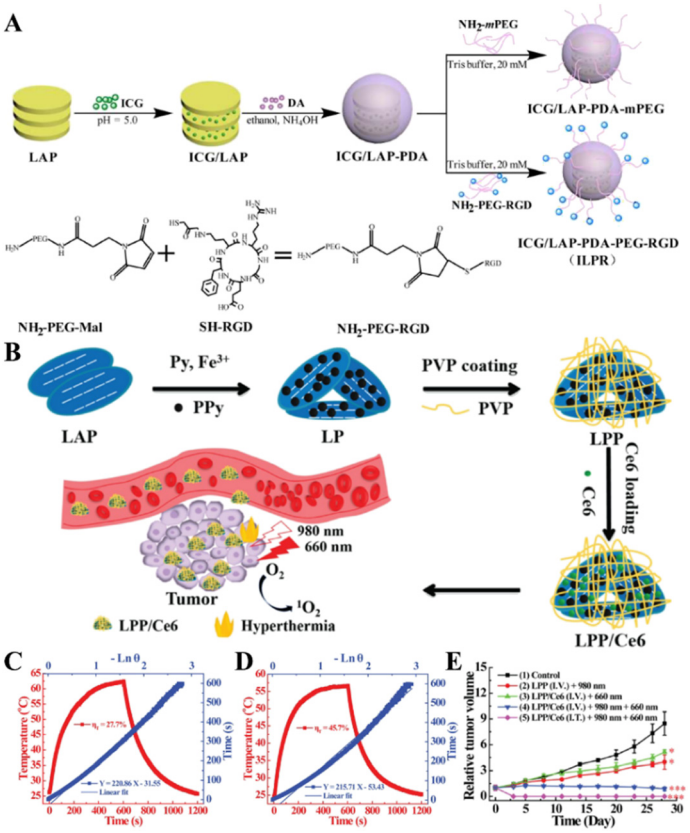

Fig. 5 (A) Schematic illustration of the synthesis of ICG/LAP–PDA–mPEG and ICG/LAP–PDA–PEG–RGD nanoparticles (NPs). Reproduced with permission.[57] Copyright 2018, MDPI. (B) Schematic diagram of the preparation of LAP NDs and Ce6 loading. Steady-state heating curves of LPP solutions under the irradiation of (C) 808 nm (1.0 W cm^{-2}) and (D) 980 nm laser (0.5 W cm^{-2}). (E) Time-dependent tumor growth profile of mice after various treatments. Reproduced with permission.[41] Copyright 2020, American Chemical Society.

PVP-coated and polypyrrole-loaded LAP NDs (for short, LPP, Fig. 5B).[41] The formed LPP nanocomplexes have good colloidal stability, cytocompatibility and photothermal conversion efficiency (Fig. 5C and D) and can be further loaded with the photosensitizer chlorin e6 (Ce6) with a high loading efficiency (denoted as LPP/Ce6). *In vivo* antitumor experiments showed that the LPP/Ce6 complexes could completely eliminate tumors through the combination of PTT and PDT (Fig. 5E).

4. LAP nanoplatforms for cancer diagnosis

Many cancer patients are diagnosed at an advanced stage when the tumors have metastasized, suffering great difficulty for complete treatment. Therefore, the early diagnosis of tumor is the key for the efficient treatment of tumors. Nanotechnology enables the development of various platforms for optical imaging, MR imaging, CT imaging, positron emission tomography (PET) imaging and single-photon emission computed tomography (SPECT) imaging for the early diagnosis of tumors.[25,58]

Among the various imaging techniques, MR imaging is an indispensable medical diagnosis method that can be used to obtain real-time 3D images of human tissues due to the differences in the water proton relaxation signals from different tissues. MR imaging can produce images with good spatial and temporal resolutions, good soft tissue contrast, and deep tissue penetration without ionizing radiation.[37] However, most of the contrast agents used in clinical practice are small molecular contrast agents based on Gd chelates that have problems such as the biological safety, short blood circulation time and inability to target cancer cells. The nano-based contrast agents constructed by combining the contrast agents with nanoplatforms can effectively prolong the blood circulation time, improve the biocompatibility, and enhance the MR contrast efficiency of the contrast agents. In a recent example, dendrimer-functionalized LAP NDs were loaded with gadolinium (Gd) for the T_1-weighted MR imaging of tumors.[59] The formed LM–G2–DTPA (Gd) nanocomplexes had a high r_1 relaxivity (2.05 mM^{-1} s^{-1}) and could be used as an efficient contrast agent for the T_1-weighted MR imaging of cancer cells *in vitro* and a xenografted tumor model *in vivo*. Besides the development of T_1-weighted MR imaging contrast agents associated with Gd chelates, LAP NDs have also been employed to construct T_2-weighted MR contrast agents associated with superparamagnetic iron oxide (Fe_3O_4) NPs. Although Fe_3O_4 NPs have a high saturation magnetization, low toxicity, large specific surface area, and strong magnetic properties, they are prone to aggregation. In a recent work, Ding *et al.* reported the development of LAP-stabilized Fe_3O_4 NPs (for short, LAP–Fe_3O_4 NPs) as a high-performance contrast agent for *in vivo* tumor MR imaging.[37] In the presence of LAP ND dispersion, Fe_3O_4 NPs were synthesized by a controlled coprecipitation method leading to the formation of LAP–Fe_3O_4 NPs (Fig. 6A). The obtained LAP–Fe_3O_4 NPs had a good colloidal stability and possessed an r_2 relaxivity of 475.9 mM^{-1} s^{-1}, which was two times higher than the LAP-free

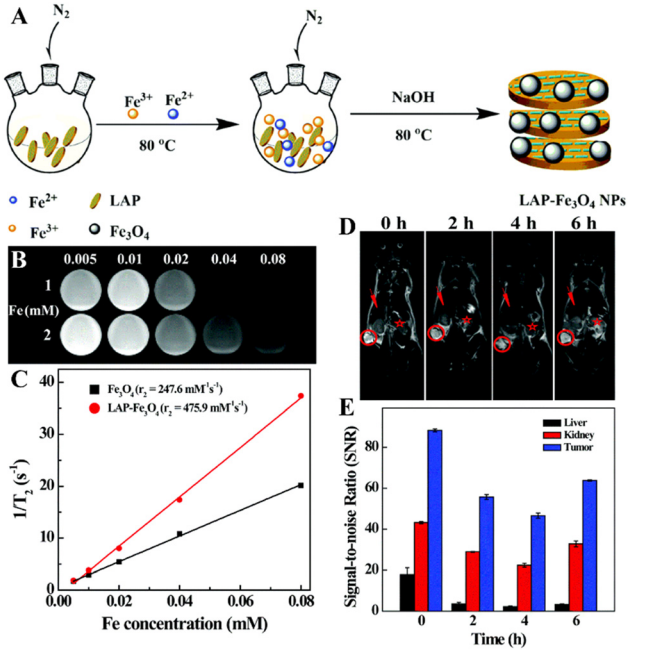

Fig. 6 (A) Schematic illustration of the synthesis of LAP–Fe_3O_4 NPs. T_2-weighted MR images (B) and linear fitting of $1/T_2$ (C) of LAP–Fe_3O_4 and Fe_3O_4 NPs at different Fe concentrations (0.005, 0.01, 0.02, 0.04, and 0.08 mM, respectively). 1 and 2 represent LAP–Fe_3O_4 and Fe_3O_4 NPs, respectively. *In vivo* T_2-weighted MR images (D) of tumor (red circle), liver (red arrow) and kidney (red star) at different time points post intravenous injection of LAP–Fe_3O_4 NPs (930 μg mL^{-1} Fe, in 0.1 mL of PBS). (E) *In vivo* MR signal-to-noise ratios (SNRs) of liver, kidney and tumor at different time points post intravenous injection of LAP–Fe_3O_4 NPs. Reproduced with permission.[37] Copyright 2016, The Royal Society of Chemistry.

Fe_3O_4 NPs (247.6 mM^{-1} s^{-1}, Fig. 6B and C), and could be used as a contrast agent for the MR imaging of cancer cells *in vitro* due to their effective cellular uptake and a xenografted tumor model through the known passive EPR effect (Fig. 6D and E). However, the rapid clearance of the reticuloendothelial system (RES) and the non-specificity of LAP–Fe_3O_4 NPs may limit the dose available for early tumor diagnosis. PEG chains are reported to reduce the interaction between NPs and macrophages.[60] In this context, biocompatible polylactic acid–PEG (PLA–PEG–COOH) was assembled onto the surface of LAP–Fe_3O_4 NPs to provide additional stability and active carboxyl groups that can be further conjugated with the FA-modified generation 2 poly(amidoamine) dendrimers (G2-FA) *via* EDC coupling chemistry.[61] Thus the prepared LAP–Fe_3O_4–PLA–PEG–G2-FA NPs had a good colloidal stability and an improved r_2 relaxivity (327.6 mM^{-1} s^{-1}), surpassing the individual Fe_3O_4 NPs (247.6 mM^{-1} s^{-1}) and the commercial products of Feridex® and Rsovist®.[62] The created hybrid NPs could specifically target cancer cell overexpressing FA receptors and be accumulated to a xenograft tumor model to generate a significant negative MR contrast enhancement at the tumor site.[61]

CT imaging has also been increasingly used because of their high spatial and density resolutions and ability to penetrate deep into tissues. In general, X-ray contrast agents with a high X-ray attenuation property are required to identify the disease

site.[63] Traditional iodine-based CT contrast agents (*e.g.*, diatrizoic acid (DTA) or iohexol) are small molecules that rapidly equilibrate between the extracellular fluid and vascular compartments in the body and are therefore rapidly cleared from the blood. To achieve the desired CT contrast enhancement, it is necessary to increase the contrast agent concentration and acquire images immediately after injection. However, high levels of iodine compounds can cause severe side effects.[64] In order to overcome these problems, Mustafa *et al.* designed DTA-modified LAP NPs for the CT imaging of main organs and tumors *in vivo*.[65] In this work, LAP NDs were silanized to render the particles with amine groups (LM–NH_2), and modified with DTA *via* EDC coupling chemistry, followed by acetylation of the remaining surface amines of the LAP NDs. The formed LM–NHAc–DTA NPs showed good stability and desirable cytocompatibility within the specified concentration range. The X-ray absorption coefficient test showed that LM–NHAc–DTA NPs had better X-ray attenuation performance than free DTA under the same iodine concentrations possibly due to the synergy of both iodine of DTA and metal elements of LAP. In addition, the acetylated LM–NHAc–DTA NPs showed an excellent performance in the CT imaging of the major organs (heart, liver, and bladder) and a tumor model *in vivo* after intravenous injection.

5. LAP nanoplatforms for cancer theranostics

The development of theranostic nanoplatforms with accurate diagnosis and effective therapy performance is crucial for precision medicine applications and to fulfil the primary goal of the personalized treatment of patients.[66] Due to the high flexibility of surface decoration and internal layer spacing incorporation, LAP NDs can be easily integrated with diagnostic and therapeutic elements to achieve accurate cancer theranostics.

In a recent study, Zhuang *et al.* reported the use of LAP NDs and PEI to establish a hybrid theranostic nanoplatform for targeted CT imaging and chemotherapy of cancer cells over-expressing the CD44 receptors.[67] In their work, the LAP NDs were first assembled with the amphiphilic copolymer PLA–PEG–COOH, and then conjugated with PEI to form LAP–PLA–PEG–PEI particles, which were used as templates to be embedded with gold (Au) NPs with a high X-ray attenuation property for CT imaging applications and to be surface modified with hyaluronic acid to serve as a targeting ligand for cancer cells with the CD44 receptor overexpression. The created LAP–PLA–PEG–PEI–$(Au^0)_{50}$–HA particles were finally loaded with DOX through physical encapsulation. The formed LAP–PLA–PEG–PEI–$(Au^0)_{50}$–HA/DOX nanocomplexes had good colloidal stability and a high drug loading efficiency of 91.0%, and could continuously release DOX in a pH-sensitive manner. The created functional nanocomplexes could not only significantly inhibit tumor growth to reduce the side effects of free DOX, but also be used as a targeted nanoprobe for specific tumor CT imaging.

In addition to CT imaging-guided tumor chemotherapy, dual mode imaging-guided phototherapy can also be achieved through the LAP-based nanoplatform. In a recent work, our group developed a novel targeted theranostic LAP nanoplatform for MR and photoacoustic (PA) imaging-guided photothermal

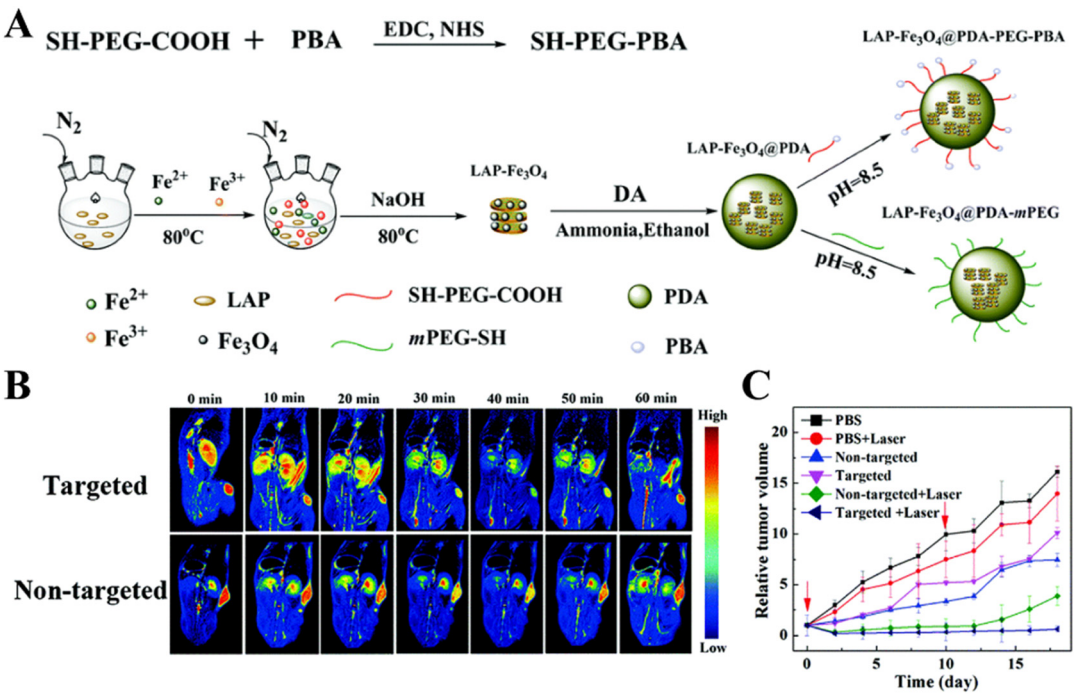

Fig. 7 (A) Schematic illustration of the synthesis of LAP–Fe_3O_4@PDA–PEG–PBA and LAP–Fe_3O_4@PDA–*m*PEG NPs. (B) MR images of the 4T1-bearing mouse model at different time points post injection of the targeted or non-targeted NPs. (C) The relative tumor volume of 4T1-bearing mice as a function of time after different treatments. Reproduced with permission.[68] Copyright 2019, The Royal Society of Chemistry.

therapy of sialic acid (SA)-overexpressing tumors (Fig. 7A).[68] In this work, LAP–Fe_3O_4 NPs with a high r_2 relaxivity were synthesized by a coprecipitation method, coated with PDA to render them with excellent photothermal effects and PA imaging properties, and then modified with PEG–PBA to introduce the tumor-targeting properties. The developed LAP–Fe_3O_4@PDA–PEG–PBA NPs showed excellent biocompatibility and photothermal conversion efficiency under near-infrared laser irradiation, and could be used for dual mode MR/PA imaging of a xenografted tumor model and complete eradication of tumors *in vivo* under NIR laser treatment (Fig. 7B and C). In addition to this, theranostic nanoplatforms combining photosensitizers and anticancer drugs have aroused considerable attention due to the real-time PA imaging capability and the synergy of chemotherapy and phototherapy to enhance the therapeutic effect. Recently, Liu *et al.* developed a PDA-coated LAP nanoplatform to efficiently load ICG and DOX, and finally modified with PEGylated RGD for PA imaging-guided chemo-phototherapy of cancer.[69] The photothermal conversion efficiency of the formed ICG/LAP–PDA–PEG-RGD/DOX nanoplatform was significantly higher than that of the free ICG, had an excellent PA imaging capability, and could release DOX in pH-sensitive and NIR laser-triggered manners. *In vitro* cell experiments showed that the ICG/LAP–PDA–PEG–RGD/DOX complexes could be taken up by 4T1 cells overexpressing $\alpha_v\beta_3$ integrin with high specificity. *In vivo* experiments with the 4T1 tumor-bearing mouse model showed that the ICG/LAP–PDA–PEG-RGD/DOX complexes could be used as a theranostic nanoprobe for PA imaging of tumor and chemo-phototherapy of tumors under NIR laser irradiation with a much stronger therapeutic effect than single-component therapy due to the synergy.

6. Conclusion and outlook

In summary, this review reports the recent advances associated with LAP ND-based platforms developed for cancer diagnosis and therapy. Due to the easy surface modification features and the interlayer spacing incorporation, LAP NDs can be loaded with therapeutic agents for targeted cancer chemotherapy, photothermal and/or photodynamic therapy, surface modified with Gd chelates or used as a stabilizer to form LAP–Fe_3O_4 NPs for MR imaging of tumors, and incorporated with both imaging and therapeutic elements for cancer theranostics such as CT imaging-guided cancer chemotherapy, dual mode imaging-guided phototherapy, or single mode imaging-guided combination therapy of tumors. The major advantages of the LAP NDs are their small size with a uniform distribution, easy surface modification, a unique interlayer space, and good biocompatibility, thus allowing for the creation of various functional platforms with excellent colloidal stability for precision cancer nanomedicine applications.

Despite the rapid development of nanotechnology associated with LAP-based platforms in the oncology domain in recent years, their applications in the field of biomedicine are still in their infancy; in particular, only a few LAP-based nanoplatforms have been assessed at the animal level. There is still a huge room left open in both basic research and clinical translation. For instance, with the understanding of the physiological properties of tumors, new treatment methods such as CDT, immunotherapy and SDT have shown broad application prospects in tumor therapy in recent years. However, the combination of the LAP nanoplatforms with these new therapies has yet to be developed. In addition, compared with the use of LAP NDs in cancer treatment, their uses in cancer diagnosis are quite limited to structural imaging modes such as CT imaging and MR imaging. It is believed that functional imaging modes such as nuclear medical imaging modes of PET and SPECT may also be developed through the use of LAP-based platforms. Furthermore, although strategies used to improve the tumor specificity of nanomedicines can be developed through improved EPR-based passive targeting and surface modification with targeting ligands, it is still challenging due to the complexity of the physiological environment and the low level of expression of the corresponding receptors in normal cells. In this context, new strategies based on the coating of cancer cell membranes on the LAP nanoplatform surface for homologous targeting or the use of immune cell-mediated delivery for tumor homing should be developed in order to further improve the selectivity, maximize the efficiency and reduce the side effects of nanomedicines. Lastly, the distribution, degradation and possible long-term toxicity of LAP-based nanoplatforms to living systems need to be intensively studied to delineate factors impacting the biosafety of the LAP-based platforms for translational medicine applications.

Conflicts of interest

The authors declare no conflicts of interest.

Acknowledgements

This study was financially supported by the National Natural Science Foundation of China (81761148028 and 22150410324), the Shanghai Education Commission through the Shanghai Leading Talents Program, and the Science and Technology Commission of Shanghai Municipality (20520710300).

Notes and references

1 H. Sung, J. Ferlay, R. L. Siegel, M. Laversanne, I. Soerjomataram, A. Jemal and F. Bray, *Ca-Cancer J. Clin.*, 2021, **71**, 209–249.
2 R. Baskar, K. A. Lee, R. Yeo and K.-W. Yeoh, *Int. J. Med. Sci.*, 2012, **9**, 193–199.
3 K. Ganesan, Y. Wang, F. Gao, Q. Liu, C. Zhang, P. Li, J. Zhang and J. Chen, *Pharmaceutics*, 2021, **13**, 1829.
4 L. Cheng, X. Wang, F. Gong, T. Liu and Z. Liu, *Adv. Mater.*, 2019, **32**, 1902333.
5 Z. Cao, B. Li, L. Sun, L. Li, Z. Xu and Z. Gu, *Small Methods*, 2019, **4**, 1900343.

6 H. Chen, Z. Gu, H. An, C. Chen, J. Chen, R. Cui, S. Chen, W. Chen, X. Chen, X. Chen, Z. Chen, B. Ding, Q. Dong, Q. Fan, T. Fu, D. Hou, Q. Jiang, H. Ke, X. Jiang, G. Liu, S. Li, T. Li, Z. Liu, G. Nie, M. Ovais, D. Pang, N. Qiu, Y. Shen, H. Tian, C. Wang, H. Wang, Z. Wang, H. Xu, J. Xu, X. Yang, S. Zhu, X. Zheng, X. Zhang, Y. Zhao, W. Tan, X. Zhang and Y. Zhao, *Sci. China: Chem.*, 2018, **61**, 1503–1552.
7 D. Banerjee, A. Cieslar-Pobuda, G. H. Zhu, E. Wiechec and H. K. Patra, *Trends Pharmacol. Sci.*, 2019, **40**, 403–418.
8 Y. Zhang, R. Lin, H. Li, W. He, J. Du and J. Wang, *Wiley Interdiscip. Rev.: Nanomed. Nanobiotechnol.*, 2018, **11**, e1519.
9 J. Wu, J. Chen, Y. Feng, H. Tian and X. Chen, *J. Gene Med.*, 2019, **21**, e3088.
10 L. E. Low, J. Wu, J. Lee, B. T. Tey, B.-H. Goh, J. Gao, F. Li and D. Ling, *J. Controlled Release*, 2020, **324**, 69–103.
11 B. He, X. Sui, B. Yu, S. Wang, Y. Shen and H. Cong, *Drug Delivery*, 2020, **27**, 1474–1490.
12 Z. Tang, P. Zhao, H. Wang, Y. Liu and W. Bu, *Chem. Rev.*, 2021, **121**, 1981–2019.
13 Z. Gong and Z. Dai, *Adv. Sci.*, 2021, **8**, 2002178.
14 S. Liu, X. Pan and H. Liu, *Angew. Chem., Int. Ed.*, 2020, **59**, 5890–5900.
15 X. Pan, H. Wang, S. Wang, X. Sun, L. Wang, W. Wang, H. Shen and H. Liu, *Sci. China: Life Sci.*, 2018, **61**, 415–426.
16 J. Ding, J. Chen, L. Gao, Z. Jiang, Y. Zhang, M. Li, Q. Xiao, S. S. Lee and X. Chen, *Nano Today*, 2019, **29**, 100800.
17 J. Huang, C. Zheng, H. Xiao, H. Huang, Y. Wang, M. Lin, J. Pang, Y. Wang, Y. Yuan and X. Shuai, *J. Controlled Release*, 2021, **340**, 259–270.
18 Q. Meng, H. Hu, X. Jing, Y. Sun, L. Zhou, Y. Zhu, B. Yu, H. Cong and Y. Shen, *J. Controlled Release*, 2021, **340**, 102–113.
19 Y. Yan, L. Zhou, Z. Sun, D. Song and Y. Cheng, *Bioact. Mater.*, 2022, **7**, 333–340.
20 Y. Fan, W. Tu, M. Shen, X. Chen, Y. Ning, J. Li, T. Chen, H. Wang, F. Yin, Y. Liu and X. Shi, *Adv. Funct. Mater.*, 2020, **30**, 1909285.
21 S. Mignani, X. Shi, K. Guidolin, G. Zheng, A. Karpus and J.-P. Majoral, *J. Controlled Release*, 2021, **337**, 356–370.
22 N. Singh, S. Son, J. An, I. Kim, M. Choi, N. Kong, W. Tao and J. S. Kim, *Chem. Soc. Rev.*, 2021, **50**, 12883–12896.
23 S. Li, L. Shang, B. Xu, S. Wang, K. Gu, Q. Wu, Y. Sun, Q. Zhang, H. Yang, F. Zhang, L. Gu, T. Zhang and H. Liu, *Angew. Chem., Int. Ed.*, 2019, **58**, 12624–12631.
24 H. Tomás, C. S. Alves and J. Rodrigues, *Nanomedicine*, 2018, **14**, 2407–2420.
25 Y. Gao, X. Shi and M. Shen, *ACS Appl. Mater. Interfaces*, 2021, **13**, 45119–45129.
26 B. Ruzicka and E. Zaccarelli, *Soft Matter*, 2011, **7**, 1268–1286.
27 S. Wang, Y. Wu, R. Guo, Y. Huang, S. Wen, M. Shen, J. Wang and X. Shi, *Langmuir*, 2013, **29**, 5030–5036.
28 Z. Cimen, S. Babadag, S. Odabas, S. Altuntas, G. Demirel and G. B. Demirel, *ACS Appl. Mater. Interfaces*, 2021, **3**, 3504–3518.
29 E. P. Rebitski, M. Darder, R. Carraro, P. Aranda and E. Ruiz-Hitzky, *New J. Chem.*, 2020, **44**, 10102–10110.
30 K. Ono, H. Hashimoto, T. Katayama, N. Ueda and K. Nagahama, *Biomacromolecules*, 2021, **22**, 4217–4227.
31 G. B. M. Câmara, R. D. M. Barbosa, F. García-Villén, C. Viseras, R. F. D. Almeida Júnior, P. R. L. Machado, C. A. Câmara, K. J. S. Farias, T. F. A. de Lima e Moura, C. A. Dreiss and F. N. Raffin, *Eur. J. Pharm. Sci.*, 2021, **163**, 105861.
32 T. Zhang, Z. Liu, H. Aslan, C. Zhang and M. Yu, *J. Mater. Chem. B*, 2020, **8**, 6429–6437.
33 T. B. Becher, M. C. P. Mendonça, M. A. de Farias, R. V. Portugal, M. B. de Jesus and C. Ornelas, *ACS Appl. Mater. Interfaces*, 2018, **10**, 21891–21900.
34 J. Li, H. Pan, S. Qiao, Y. Li, J. Wang, W. Liu and W. Pan, *Int. J. Biol. Macromol.*, 2019, **134**, 63–72.
35 P. A. Wheeler, J. Wang, J. Baker and L. J. Mathias, *Chem. Mater.*, 2005, **17**, 3012–3018.
36 Y. Wu, K. Li, L. Kong, Y. Tang, G. Li, W. Jiang, M. Shen, R. Guo, Q. Zhao and X. Shi, *Bioconjugate Chem.*, 2020, **31**, 2404–2412.
37 L. Ding, Y. Hu, Y. Luo, J. Zhu, Y. Wu, Z. Yu, X. Cao, C. Peng, X. Shi and R. Guo, *Biomater. Sci.*, 2016, **4**, 474–482.
38 H. Abdel Mageed, K. Van Der Speeten and P. Sugarbaker, *Surg. Oncol.*, 2022, **40**, 101676.
39 C. Tang, H. Liu, Y. Fan, J. He, F. Li, J. Wang and Y. Hou, *Front. Pharmacol.*, 2021, **12**, 778973.
40 C. Zhang, W. Sun, Y. Wang, F. Xu, J. Qu, J. Xia, M. Shen and X. Shi, *ACS Appl. Mater. Interfaces*, 2020, **12**, 9107–9117.
41 H. Wu, W. Wang, Z. Zhang, J. Li, J. Zhao, Y. Liu, C. Wu, M. Huang, Y. Li and S. Wang, *ACS Appl. Mater. Interfaces*, 2019, **12**, 390–399.
42 H. Yang, B. Xu, S. Li, Q. Wu, M. Lu, A. Han and H. Liu, *Small*, 2021, **17**, 2007090.
43 Y. Liang, Z. Liu, P. Wang, Y. Li, R. Wang and S. Xie, *J. Controlled Release*, 2021, **336**, 396–409.
44 B. Zhou, B. Wu, J. Wang, Q. Qian, J. Wang, H. Xu, S. Yang, P. Feng, W. Chen, Y. Li, J. Jiang and B. Han, *Colloids Surf., B*, 2018, **163**, 284–290.
45 Z. Su, S. Dong, S.-C. Zhao, K. Liu, Y. Tan, X. Jiang, Y. G. Assaraf, B. Qin, Z. Chen and C. Zou, *Drug Resist. Updates*, 2021, **58**, 100777.
46 M. Gonçalves, P. Figueira, D. Maciel, J. Rodrigues, X. Qu, C. Liu, H. Tomás and Y. Li, *Acta Biomater.*, 2014, **10**, 300–307.
47 G. Wang, D. Maciel, Y. Wu, J. Rodrigues, X. Shi, Y. Yuan, C. Liu, H. Tomás and Y. Li, *ACS Appl. Mater. Interfaces*, 2014, **6**, 16687–16695.
48 S. Xiao, R. Castro, D. Maciel, M. Gonçalves, X. Shi, J. Rodrigues and H. Tomás, *Mater. Sci. Eng., C*, 2016, **60**, 348–356.
49 J. Wang, G. Wang, Y. Sun, Y. Wang, Y. Yang, Y. Yuan, Y. Li and C. Liu, *RSC Adv.*, 2016, **6**, 31816–31823.
50 T. Jiang, C. Zhang, W. Sun, X. Cao, G. Choi, J. H. Choy, X. Shi and R. Guo, *Chem. - Eur. J.*, 2020, **26**, 2470–2477.
51 T. Jiang, G. Chen, X. Shi and R. Guo, *Polymers*, 2019, **11**, 137.
52 G. Chen, D. Li, J. Li, X. Cao, J. Wang, X. Shi and R. Guo, *New J. Chem.*, 2015, **39**, 2847–2855.
53 Y. Yang, J. Y. Li, F. Chen, S. Qiao, Y. J. Li and W. S. Pan, *AAPS PharmSciTech*, 2020, **21**, 5.

54 S. Son, J. H. Kim, X. Wang, C. Zhang, S. A. Yoon, J. Shin, A. Sharma, M. H. Lee, L. Cheng, J. Wu and J. S. Kim, *Chem. Soc. Rev.*, 2020, **49**, 3244–3261.
55 Z. Ouyang, D. Li, Z. Xiong, C. Song, Y. Gao, R. Liu, M. Shen and X. Shi, *ACS Appl. Mater. Interfaces*, 2021, **13**, 6069–6080.
56 H. Ma and M. Xue, *J. Mater. Chem. A*, 2021, **9**, 17569–17591.
57 F. Xu, M. Liu, X. Li, Z. Xiong, X. Cao, X. Shi and R. Guo, *Nanomaterials*, 2018, **8**, 347.
58 S. Eom, G. Choi, H. Nakamura and J.-H. Choy, *Bull. Chem. Soc. Jpn.*, 2020, **93**, 1–12.
59 R. Mustafa, B. Zhou, J. Yang, L. Zheng, G. Zhang and X. Shi, *RSC Adv.*, 2016, **6**, 95112–95119.
60 J. L. Perry, K. G. Reuter, M. P. Kai, K. P. Herlihy, S. W. Jones, J. C. Luft, M. Napier, J. E. Bear and J. M. DeSimone, *Nano Lett.*, 2012, **12**, 5304–5310.
61 L. Ding, R. Wang, Y. Hu, F. Xu, N. Zhang, X. Cao, X. Wang, X. Shi and R. Guo, *Appl. Clay Sci.*, 2020, **186**, 105447.
62 J. Wahsner, E. M. Gale, A. Rodríguez-Rodríguez and P. Caravan, *Chem. Rev.*, 2018, **119**, 957–1057.
63 J. Zhu, L. Zheng, S. Wen, Y. Tang, M. Shen, G. Zhang and X. Shi, *Biomaterials*, 2014, **35**, 7635–7646.
64 C. Peng, L. Zheng, Q. Chen, M. Shen, R. Guo, H. Wang, X. Cao, G. Zhang and X. Shi, *Biomaterials*, 2012, **33**, 1107–1119.
65 R. Mustafa, Y. Hu, J. Yang, J. Chen, H. Wang, G. Zhang and X. Shi, *RSC Adv.*, 2016, **6**, 57490–57496.
66 W. Cai, C.-C. Chu, G. Liu and Y.-X. J. Wáng, *Small*, 2015, **11**, 4806–4822.
67 Y. Zhuang, L. Zhao, L. Zheng, Y. Hu, L. Ding, X. Li, C. Liu, J. Zhao, X. Shi and R. Guo, *ACS Biomater. Sci. Eng.*, 2017, **3**, 431–442.
68 M. Liu, J. Zhang, X. Li, C. Cai, X. Cao, X. Shi and R. Guo, *J. Mater. Chem. B*, 2019, **7**, 3856–3864.
69 R. Liu, F. Xu, L. Wang, M. Liu, X. Cao, X. Shi and R. Guo, *Nanomaterials*, 2021, **11**, 394.